Atmos. Chem. Phys., 9, 5933–5948, 2009
www.atmos-chem-phys.net/9/5933/2009/

Atmospheric Chemistry and Physics

Parameterizing the competition between homogeneous and heterogeneous freezing in ice cloud formation – polydisperse ice nuclei

D. Barahona[1] **and A. Nenes**[1,2]

[1]School of Chemical and Biomolecular Engineering, Georgia Institute of Technology, USA
[2]School of Earth and Atmospheric Sciences, Georgia Institute of Technology, USA

Received: 29 March 2009 – Published in Atmos. Chem. Phys. Discuss.: 5 May 2009
Revised: 28 July 2009 – Accepted: 5 August 2009 – Published: 19 August 2009

Abstract. This study presents a comprehensive ice cloud formation parameterization that computes the ice crystal number, size distribution, and maximum supersaturation from precursor aerosol and ice nuclei. The parameterization provides an analytical solution of the cloud parcel model equations and accounts for the competition effects between homogeneous and heterogeneous freezing, and, between heterogeneous freezing in different modes. The diversity of heterogeneous nuclei is described through a nucleation spectrum function which is allowed to follow any form (i.e., derived from classical nucleation theory or from observations). The parameterization reproduces the predictions of a detailed numerical parcel model over a wide range of conditions, and several expressions for the nucleation spectrum. The average error in ice crystal number concentration was $-2.0\pm8.5\%$ for conditions of pure heterogeneous freezing, and, $4.7\pm21\%$ when both homogeneous and heterogeneous freezing were active. The formulation presented is fast and free from requirements of numerical integration.

1 Introduction

Ice clouds play a key role in rain production (e.g., Lau and Wu, 2003), heterogeneous chemistry (Peter, 1997), stratospheric water vapor circulation (Hartmann et al., 2001), and the radiative balance of the Earth (Liou, 1986). Representation of ice clouds in climate and weather prediction models remains a challenge due to the limited understanding of ice cloud formation processes (e.g., Lin et al., 2002; Baker and Peter, 2008), and the difficulties associated with the remote sensing of ice clouds (Waliser et al., 2009). Anthropogenic activities can potentially influence ice cloud formation and evolution by altering the concentration and composition of precursor aerosols (Seinfeld, 1998; Penner et al., 1999; Minnis, 2004; Kärcher et al., 2007), which may result in a potentially important indirect effect (e.g., Kärcher and Lohmann, 2003), the sign and magnitude of which however is highly uncertain.

Ice clouds form by homogeneous freezing of liquid droplets or heterogeneous freezing upon ice nuclei, (IN) (e.g., Pruppacher and Klett, 1997). Observational data show that the two freezing mechanisms are likely to interact during cloud formation (DeMott et al., 2003a, b; Haag et al., 2003b; Prenni et al., 2007); their relative contribution is however a strong function of IN, aerosol concentration, and cloud formation conditions (Gierens, 2003; Kärcher et al., 2006; Barahona and Nenes, 2009). IN tend to freeze early during cloud formation, depleting water vapor supersaturation and hindering the freezing of IN with high freezing thresholds and the homogeneous freezing of liquid droplets (e.g., DeMott et al., 1997; Koop et al., 2000). Although numerous aerosol species have been identified as active IN, dust, soot, and organic particles are thought to be the most relevant for the atmosphere (DeMott et al., 2003a; Sassen et al., 2003; Archuleta et al., 2005; Möhler et al., 2005; Field et al., 2006; Kanji et al., 2008; Phillips et al., 2008). Assessment of the indirect effect resulting from perturbations in the background concentrations of IN requires a proper characterization of the spatial distribution of potential IN species and their freezing efficiencies (i.e., the aerosol freezing fraction). The large uncertainty in ice cloud indirect forcing is associated with

Correspondence to: A. Nenes
(athanasios.nenes@gatech.edu)

incomplete understanding of these factors which is evident by the large predictive uncertainty of aerosol-cloud parameterizations (Phillips et al., 2008; Eidhammer et al., 2009).

Several approaches have been proposed to parameterize ice cloud formation in atmospheric models. Empirical correlations derived from field campaigns are most often employed to express IN concentrations (e.g., Meyers et al., 1992; DeMott et al., 1998) as a function of temperature, T, and supersaturation over ice, s_i. These expressions are simple but only provide the availability of IN over a limited spatial region. A more comprehensive expression was developed by Phillips et al. (2008), who combined data from several field campaigns to estimate the contribution of individual aerosol species to the total IN concentration.

Empirical parameterizations are incomplete, as they provide only IN concentrations. Calculation of ice crystal number concentration, N_c, requires the knowledge of cloud supersaturation and therefore the usage of a dynamical framework. Liu and Penner (2005) considered this, and used numerical solutions from a cloud parcel model to correlate N_c to cloud formation conditions (i.e., T, p, V) and the number concentration of individual aerosol species (dust, soot, and sulfate). Although a computationally efficient approach, these correlations are restricted to (largely unconstrained) assumptions regarding the nature of freezing (i.e., the estimation of freezing efficiencies), the size distributions of dust, soot, and sulfate, the mass transfer (i.e., deposition) coefficient of water vapor onto crystals, and, the active freezing mechanisms. Kärcher et al. (2006) proposed a physically based approach to parameterize cirrus cloud formation combining solutions for the pure homogeneous freezing (Kärcher and Lohmann, 2002b), and heterogeneous freezing (Kärcher and Lohmann, 2003) into a numerical scheme. Although this approach includes all known relevant factors that determine N_c, it may be computationally intensive; thus, its application is limited to cases where IN can be characterized by a few, well defined, freezing thresholds. Even if many cases of atmospheric aerosol can be described this way, it may not be adequate, as even single class aerosol populations usually exhibit a distribution of freezing thresholds (e.g., Meyers et al., 1992; Möhler et al., 2006; Marcolli et al., 2007; Kanji et al., 2008; Phillips et al., 2008; Vali, 2008; Welti et al., 2009). Barahona and Nenes (2009) developed an analytical parameterization that combines homogeneous and heterogeneous freezing within a single expression. Although very fast and with low error (6±33%), this approach is limited to cases where the IN population can be characterized by a single freezing threshold.

This work presents a new physically-based, analytical and computationally efficient framework to parameterize ice cloud formation. The new scheme allows the usage of both empirical and theoretical IN data in a simple dynamical framework, and can consider the spectral variability in aerosol and IN composition. The new parameterization builds upon the frameworks of Barahona and Nenes (2008, 2009) that combine homogeneous and heterogeneous mechanisms of ice formation, and explicitly resolves the dependency of N_c on conditions of cloud formation (i.e., T, p, V), aerosol number and size, and the freezing characteristics of the IN.

2 Description of the ice nucleation spectrum

Modeling of ice cloud formation requires a function describing the number concentration of crystals frozen from an aerosol population (i.e., the aerosol freezing fraction) at some temperature, T, and supersaturation, s_i. The function, known as the "nucleation spectrum", is closely related to the nucleation rate coefficient, J, and the freezing probability, P_f. Theoretical studies (e.g., Lin et al., 2002; Khvorostyanov and Curry, 2009) and laboratory experiments (e.g., Tabazadeh et al., 1997a; Koop et al., 2000; Hung et al., 2002; Haag et al., 2003a, b) suggest that J becomes substantially large around some threshold T and s_i (Pruppacher and Klett, 1997). Decreasing T (or increasing s_i) beyond this level exponentially increases J so that (unless s_i is depleted by water vapor deposition onto growing ice crystals) the probability of freezing, P_f eventually becomes unity (Pruppacher and Klett, 1997; Lin et al., 2002; Khvorostyanov and Curry, 2004; Monier et al., 2006; Barahona and Nenes, 2008). Observations have confirmed this for homogeneous freezing of aqueous droplets, where the threshold s_i and T is confined within a very narrow range of values (Heymsfield and Sabin, 1989; DeMott et al., 1994; Pruppacher and Klett, 1997; Tabazadeh et al., 1997b; Chen et al., 2000; Cziczo and Abbatt, 2001; Khvorostyanov and Curry, 2004) and depends primarily on the water activity within the liquid phase (Koop et al., 2000).

Heterogeneous freezing is different from homogeneous freezing in that it exhibits a broad range of freezing thresholds, even for aerosol of the same type (e.g., Pruppacher and Klett, 1997; Zuberi et al., 2002; Archuleta et al., 2005; Abbatt et al., 2006; Field et al., 2006; Möhler et al., 2006; Marcolli et al., 2007; Eastwood et al., 2008; Kanji et al., 2008; Khvorostyanov and Curry, 2009). Field campaign data (Meyers et al., 1992; DeMott et al., 1998) and laboratory studies (Field et al., 2006; Möhler et al., 2006; Zobrist et al., 2008; Welti et al., 2009) show that for s_i values larger than the threshold s_i, the aerosol freezing fraction (i.e., P_f) is below unity, increasing with s_i much more slowly than suggested by theory (e.g., Khvorostyanov and Curry, 2005; Phillips et al., 2008; Eidhammer et al., 2009). This discrepancy can be reconciled by assuming that the heterogeneous nucleation rate depends on the local conditions adjacent to individual nucleation sites, rather than on the average characteristics of the aerosol population (i.e., the "singular hypothesis" (e.g., Fletcher, 1969; Vali, 1994)). Freezing occurs instantaneously when a threshold s_i and T associated with a nucleation site are reached; thus a distribution of active nucleation sites on the aerosol particles would

Table 1. Cumulative freezing spectra considered in this study. The functions $H_{\rm soot}(s_i, T)$ and $H_{\rm dust}(s_i, T)$ for PDA08 are defined in Phillips et al. (2008).

Spectrum	$N_{\rm het}(s_i)$ ($\rm m^{-3}$)
Meyers et al. (1992), MY92	$10^3 e^{-0.639+12.96 s_i}$
Phillips et al. (2007), PDG07	$60 e^{-0.639+12.96 s_i} \quad 243<T<268$ $10^3 e^{-0.388+3.88 s_i} \quad 190<T\leq 243$
Phillips et al. (2008), PDA08	$N_{\rm dust}\left[1-\exp\left(-\frac{2}{3} H_{\rm dust}(s_i, T)\frac{N_{\rm het,PDG07}}{7.92\times 10^4}\right)\right]$ $+N_{\rm soot}\left[1-\exp\left(-\frac{1}{3} H_{\rm soot}(s_i, T)\frac{N_{\rm het,PDG07}}{1.04\times 10^6}\right)\right]$
Classical Nucleation Theory (Sect. 2.2), CNT	$0.05\left[\min\left(\frac{s_i}{0.2} N_{\rm dust} e^{-0.0011 k_{\rm hom}(0.2-s_i)},\ N_{\rm dust}\right)+\right.$ $\left.\min\left(\frac{s_i}{0.3} N_{\rm soot} e^{-0.039 k_{\rm hom}(0.3-s_i)},\ N_{\rm soot}\right)\right]$

result in a distribution of freezing thresholds (Marcolli et al., 2007; Zobrist et al., 2007; Vali, 2008; Eidhammer et al., 2009; Khvorostyanov and Curry, 2009). The aerosol freezing fraction is then related to the density of active nucleation sites (which generally depends on particle history and chemical composition (Pruppacher and Klett, 1997; Abbatt et al., 2006)) and to the surface area and number concentration of the aerosol population. Vali (1994, 2008) have argued that $P_f<1$ for each active nucleation site, which may arise if the active sites exhibit transient activity; this implies a temporal dependency of P_f which is however second order on the freezing threshold distribution (Vali, 2008; Khvorostyanov and Curry, 2009).

Experimental studies and field campaign data (e.g., Möhler et al., 2006; Phillips et al., 2008) show that at constant T, the aerosol freezing fraction is well represented by a continuous function of s_i, which results from the diversity of active nucleation sites that may be available in the insoluble aerosol population (Pruppacher and Klett, 1997). If sufficient time is allowed so that transient effects vanish (i.e., P_f is at its maximum), then the "nucleation spectrum" can be defined as,

$$n_s(s_i, T, p, ...) = \left.\frac{\partial N_{\rm het}(s_i, T, p, ...)}{\partial s_i}\right|_{T,p,...} \quad (1)$$

where $N_{\rm het}(s_i, T, p, ...)$ is the crystal number concentration produced by heterogeneous freezing. The subscripts on the right hand side of Eq. (1) indicate that all other state variables (T, p, aerosol concentrations) remain constant when the nucleation spectrum is measured or computed with theory. Therefore, for the remainder of this study, $N_{\rm het}(s_i, T, p, ...)$ is represented as $N_{\rm het}(s_i)$ ($n_s(s_i)$ in its differential form), assuming an implicit dependency on other state variables.

2.1 Empirical IN spectra

Developing an ice formation parameterization requires the knowledge of the IN nucleation spectrum in its differential $n_s(s_i)$, or cumulative form, $N_{\rm het}(s_i)$; these can be obtained empirically from field campaign data (Meyers et al., 1992; Phillips et al., 2008), laboratory experiments (e.g., Möhler et al., 2006; Welti et al., 2009) or from nucleation theory (Sect. 2.2). The simplest form for $n_s(s_i)$ arises by assuming that IN concentrations depend solely on s_i; characteristic examples are the formulations of Meyers et al. (1992, MY92, Table 1) and the background spectrum of Phillips et al. (2007, PDG07, Table 1). MY92 is derived from in-situ measurements of IN concentrations for T between 250 and 266 K and s_i between 2 and 25%. PDG07 is derived from MY92 (after applying a scaling factor to account for the height dependency of IN concentration) and the data of DeMott et al. (2003a). A more comprehensive formulation, considering (in addition to s_i and T) the surface area contribution from different aerosol types (i.e., dust, organic carbon, and soot) and freezing modes (i.e., deposition and immersion), was presented by Phillips et al. (2008, PDA08). PDA08 is developed using IN and aerosol concentration measurements from several field campaigns.

2.2 IN spectra from classical nucleation theory

Theoretical arguments can also be used to obtain an approximate form for the nucleation spectrum. Classical nucleation theory (CNT) suggests that the nucleation rate at two s_i thresholds can be related as (Pruppacher and Klett, 1997; Khvorostyanov and Curry, 2004)

$$J(s_{i,1}) \approx J(s_{i,2}) \exp\left[-k(T)(s_{i,2}-s_{i,1})\right] \quad (2)$$

where $J(s_{i,1})$ and $J(s_{i,2})$ are the nucleation rate coefficients at $s_{i,1}$ and $s_{i,2}$, respectively; $k(T)$ is a proportionality constant depending on T. Using this, Barahona and Nenes (2008) showed that for pure homogeneous freezing the nucleation spectrum, $N_{\rm hom}(s_i)$, can be approximated as,

$$N_{\rm hom}(s_i) \approx N_o \frac{J_{\rm hom}(s_{\rm hom})\bar{v}_o}{\alpha V\, k_{\rm hom}} \frac{1}{(s_{\rm hom}+1)} \exp\left[-k_{\rm hom}(s_{\rm hom}-s_i)\right] \quad (3)$$

where $J_{\rm hom}(s_{\rm hom})$ is the homogenous nucleation rate coefficient at the homogeneous freezing threshold, $s_{\rm hom}$; N_o and $\bar{v}_o$ are the number concentration and mean volume of the droplet population, respectively, and $k_{\rm hom}=(s_{\rm hom}-s_i)^{-1}\ln\frac{J_{\rm hom}(s_{\rm hom})}{J_{\rm hom}(s_i)}$. Equation (3) can be extended to describe heterogeneous nucleation by replacing $k_{\rm hom}$ with a heterogeneous nucleation analog, $k(T)$ (e.g., Pruppacher and Klett, 1997; Khvorostyanov and Curry, 2004, 2009),

$$k(T) = k_{\rm hom} f_h \tag{4}$$

where $f_h \approx \frac{1}{4}\left(m^3-3m+2\right)$, $m=\cos(\theta)$ and θ is the IN-water contact angle (Fletcher, 1959). Replacing $k_{\rm hom}$ in Eq. (3) with $k(T)$ from Eq. (4), $s_{\rm hom}$ with the heterogeneous freezing threshold, $s_{h,j}$, and, generalizing to an external mixture of *nsp* IN populations, we obtain

$$N_{\rm het}(s_i) \approx \sum_{j=1,nsp} \min\left\{e_{f,j}\,N_{a,j}\exp\left[-k_{\rm hom} f_{h,j}(s_{h,j}-s_i)\right]\ ,\ e_{f,j}\,N_{a,j}\right\} \tag{5}$$

where $s_{h,j}$ is the freezing threshold of the j-th IN population, and, $N_{a,j}$ is the corresponding aerosol number concentration; $s_{h,j}$ is associated with the onset of large nucleation rates at which the aerosol freezing fraction reaches a maximum. $e_{f,j} \approx \left[C\frac{J_{h,j}(s_{h,j})\bar{\Omega}_j}{\alpha V\, k(T)}\frac{1}{(s_{h,j}+1)}\right]$ is the freezing efficiency of the j-th population, where $J_{h,j}(s_{h,j})$ is the heterogeneous nucleation rate coefficient at $s_{h,j}$, and C depends on the mean surface area of the j-th aerosol population, $\bar{\Omega}_j$.

Nucleation spectra based on CNT (and therefore on the stochastic hypothesis (Pruppacher and Klett, 1997)) depend on t, which is evident in Eq. (5) as $e_{f,j} \propto \frac{J(s_{h,j})}{V}$. To be consistent with Eq. (1), the temporal dependency in Eq. (5) should vanish, which implies that $e_{f,j} \neq f(t)$. Assuming that enough time is allowed for heterogeneous freezing during IN measurements (used to constrain the parameters of CNT), the stochastic component of CNT is small, and the resulting nucleation spectra would practically be time-independent, hence consistent with Eq. (1).

The exponential form of Eq. (5) is in agreement with experimental studies (e.g., Möhler et al., 2006). Equation (5) however requires the knowledge of $e_{f,j}$ which in this study is treated as an empirical parameter and used to constrain the maximum freezing fraction of the aerosol population (in reality, $e_{f,j}$ is a function of T, aerosol composition and size, and is analyzed in a companion study). Values for $e_{f,j}$, $s_{h,j}$, and θ_j used in this study (Sect. 4.1, Table 1) are selected from the literature. Complete characterization of the nucleation spectra using nucleation theory requires the usage of probability distributions for θ_j and $s_{h,j}$ (e.g., Marcolli et al., 2007; Khvorostyanov and Curry, 2009). Although this can in principle be included in Eq. (5), little is known on the formulation of such probability distributions and is not considered here.

3 Formulation of the parameterization

The parameterization is based on the framework of an ascending Lagrangian parcel. At any height during the parcel ascent, supersaturation with respect to ice, s_i, develops and the ice crystal size distribution is determined by heterogeneous freezing of IN, homogeneous freezing of droplets, and growth of existing ice crystals. The solution when homogeneous freezing is the only mechanism active is presented in Barahona and Nenes (2008). The general solution for pure heterogeneous, and, combined homogeneous-heterogeneous freezing is presented in the following sections.

3.1 The ice parcel equations

In the initial stages of cloud formation s_i increases monotonically due to cooling from expansion; growth of crystals, frozen either homogeneously or heterogeneously, increasingly depletes water vapor, up to some level where s_i reaches a maximum, $s_{\rm max}$ (because depletion balances the s_i increase from cooling). At any given time, the state of the cloud is determined by the coupled system of equations (Barahona and Nenes, 2009)

$$w_i(t) = \frac{\rho_i}{\rho_a}\frac{\pi}{6}\int ... \int_X D_c^3 n_c(D_c, D_{\rm IN}, m_{1,...,nx}, t)\,dD_c\,dD_{\rm IN}\,dm_{1,...,nx} \tag{6}$$

$$\frac{ds_i}{dt} = \alpha V(1+s_i) - \beta\frac{dw_i}{dt} \tag{7}$$

$$\frac{dw_i}{dt} = \frac{\rho_i}{\rho_a}\frac{\pi}{2}\int ... \int_X D_c^2\frac{dD_c}{dt} n_c(D_c, D_{\rm IN}, m_{1,...,nx}, t)\,dD_c\,dD_{\rm IN}\,dm_{1,...,nx} \tag{8}$$

$$\frac{dD_c}{dt} = \frac{s_i}{\Gamma_1 D_c + \Gamma_2} \tag{9}$$

where $\frac{dw_i}{dt}$ is the rate of water vapor deposition on the ice crystals and V is the updraft velocity. D_c and $D_{\rm IN}$ are the volume-equivalent diameter of the ice crystals and IN, respectively (for homogeneous nucleation, $D_{\rm IN}$ is replaced by the size of cloud droplets), $m_{1,...,nx}$ collectively represents the mass fractions of the nx chemical species present in the aerosol population (all other symbols are defined in Appendix C). $n_c\left(D_c, D_{\rm IN}, m_{1,...,nx}, t\right)$ is the number distribution of the ice crystals; therefore $n_c(D_c, D_{\rm IN}, m_{1,...,nx}, t)dD_c dD_{\rm IN} dm_{1,...,nx}$ represents the number concentration of ice crystals with sizes in the range (D_c, D_c+dD_c), made from an aerosol particle in the size range $(D_{\rm IN}, D_{\rm IN}+dD_{\rm IN})$, and with composition defined by the interval $(m_{1,...,nx}, m_{1,...,nx}+dm_{1,...,nx})$. X in Eqs. (6) and (8) is the domain of integration and spans over all the values of D_c, $D_{\rm IN}$, and $m_{1,...,nx}$ for which $n_c(D_c, D_{\rm IN}, m_{1,...,nx}, t)$

is defined. The calculation of $w_i(t)$ and $\frac{dw_i}{dt}$ requires the knowledge of $n_c(D_c, D_{\rm IN}, m_{1,\ldots,nx}, t)$, therefore an equation describing the evolution of $n_c(D_c, D_{\rm IN}, m_{1,\ldots,nx}, t)$ should be added to Eqs. (7) to (9). The coupling between n_c, D_c, and s_i in Eqs. (7) to (9) precludes a closed analytical solution and are numerically integrated (e.g., Lin et al., 2002, and references therein; Monier et al., 2006; Barahona and Nenes, 2008).

The main parameter of interest resulting from the solution of Eqs. (7) to (9) is the ice crystal number concentration, $N_c = N_{\rm hom} + N_{\rm het}$, where $N_{\rm hom}$ and $N_{\rm het}$ are the ice crystal number concentrations from homogeneous and heterogeneous freezing, respectively. $N_{\rm hom}$ can be treated using the analytical approach of Barahona and Nenes (2008), while $N_{\rm het}$ is equal to the IN that freeze, i.e., $N_{\rm het}$ at $s_{\rm max}$. Therefore, determining N_c requires the computation of $s_{\rm max}$.

3.2 Determining $s_{\rm max}$ and $N_{\rm het}$

$s_{\rm max}$ and $N_{\rm het}$ are determined by solving for the supersaturation that is a root of Eq. (7). This is turn is accomplished by manipulating Eq. (7) so that the contribution of nucleation and growth to the evolution of the ice crystal population is decoupled. The root is then analytically determined for freezing of a monodisperse, chemically homogenous, ice crystal population based on the approach of Barahona and Nenes (2009). The monodisperse solution is then generalized for a polydisperse, heterogeneous IN population by introducing the characteristic freezing threshold and size of the ice crystal population.

The size of ice crystals at any time after freezing and growth is given by integration of Eq. (9), assuming negligible non-continuum effects on mass transfer; i.e., $\Gamma_1 \gg \Gamma_2$ (Appendix B), and, $\frac{dD_c}{dt} \approx \frac{s_i}{\Gamma_1 D_c}$ (Barahona and Nenes, 2008),

$$D_c(t, s_i) = \left(D_{\rm IN}^2 + \frac{1}{\Gamma_1} \int_{s_o'}^{s_i} \frac{s}{ds/dt} ds \right)^{1/2} \tag{10}$$

where $D_{\rm IN}$ is the initial size of the ice crystals at the moment of freezing, and, s_o' is their freezing threshold (Barahona and Nenes, 2008), which depends on composition and size (Sect. 2). A chemically-heterogeneous, polydisperse IN population can thus be treated as the superposition of monodisperse, chemically-homogeneous IN classes, each with their respective s_o'; Eq. (10) can then be applied seperately to each "IN class" of size and composition.

Equation (10) can be simplified assuming that $\frac{1}{\Gamma_1} \int_{s_o'}^{s_i} \frac{s}{ds/dt} ds \gg D_{\rm IN}^2$, which means that the growth experienced by crystals beyond the point of freezing is much larger than their initial size (e.g., Kärcher and Lohmann, 2002b; Nenes and Seinfeld, 2003; Khvorostyanov and Curry, 2005; Monier et al., 2006; Barahona and Nenes, 2009), and is justified given that typical crystal sizes, $D_c > 20\,\mu$m, are much larger than the typical $D_{\rm IN} \sim 1\,\mu$m found in the upper troposphere (e.g., Heymsfield and Platt, 1984; Gayet et al., 2004). Equation (10) is further simplified by considering that the thermodynamic driving force for ice crystal growth (i.e., the difference between s_i and the equilibrium supersaturation) is usually large ($s_{\rm max}$ generally above 20% (e.g., Lin et al., 2002; Haag et al., 2003b)). This suggests that crystal growth rates would be limited by water vapor mass transfer rather than by s_i (confirmed by parcel model simulations). D_c is therefore a strong function of the crystal residence time in the parcel and weakly dependent on s_i. The limits of the integral in Eq. (10) imply that the crystal residence time is mainly a function of the difference $s_i - s_o'$; Eq. (10) therefore can be rewritten as

$$D_c(t, s_i) \approx D_c(s_i - s_o') \tag{11}$$

where $D_c(s_i - s_o')$ signifies that D_c is a function of $s_i - s_o'$.

Equations (1) and (11) suggest that Eq. (6) can be written in terms of s_i and s_o',

$$\begin{aligned} w_i(s_i) &= \frac{\pi}{6} \frac{\rho_i}{\rho_a} \int_0^{s_i} D_c^3(s_i - s_o')\, n_s(s_o')\, ds_o' \\ &= \frac{\pi}{6} \frac{\rho_i}{\rho_a} \left[D_c^3 \otimes n_s \right](s_i) \end{aligned} \tag{12}$$

where $\otimes$ represents the half-convolution product (Appendix A). Taking the derivative of Eq. (12) and substitution into Eq. (7) gives,

$$\frac{ds_i}{dt} = \alpha V (1 + s_i) - \beta \frac{\rho_i}{\rho_a} \frac{\pi}{2} \left[D_c^2 \frac{dD_c}{dt} \otimes n_s \right](s_i) \tag{13}$$

Equation (13) is a simplified supersaturation balance equation used in place of Eq. (7), the root of which (i.e., $\frac{ds_i}{dt} = 0$) gives $s_{\rm max}$,

$$\alpha V (1 + s_{\rm max}) = \beta \frac{\rho_i}{\rho_a} \frac{\pi}{2} \left[D_c^2 \frac{dD_c}{dt} \otimes n_s \right](s_{\rm max}) \tag{14}$$

$D_c^2 \frac{dD_c}{dt}$, defined in Eq. (9), can be simplified using the approximation developed in Appendix B, i.e., $\frac{D_c^2 s_{\rm max}}{\Gamma_1 D_c + \Gamma_2} \approx \frac{s_{\rm max}}{\Gamma_1} D_c\, e^{-\frac{2}{\lambda s_{\rm max}}}$. Introducing Eq. (B6) into Eq. (14) and rearranging gives,

$$\frac{\alpha V \Gamma_1}{\beta \frac{\rho_i}{\rho_a} \frac{\pi}{2}} \frac{1 + s_{\rm max}}{s_{\rm max}} e^{\frac{2}{\lambda s_{\rm max}}} = \left[D_c \otimes n_s \right](s_{\rm max}) \tag{15}$$

Equation (15) holds regardless of the form of $n_s(s_i)$, and can be applied to a monodisperse, chemically-homogeneous IN population, for which all ice crystals freeze at a characteristic threshold, $s_{\rm char}$. $n_s(s_i)$ is thus a delta function about $s_{\rm char}$, $\delta(s - s_{\rm char})$. Substitution into Eq. (15) gives

$$\begin{aligned} &\frac{\alpha V \Gamma_1}{\beta \frac{\rho_i}{\rho_a} \frac{\pi}{2}} \frac{1 + s_{\rm max}}{s_{\rm max}} e^{\frac{2}{\lambda s_{\rm max}}} = \\ &\qquad N_{\rm het}(s_{\rm max}) \int_{s_{char}}^{s_{\rm max}} D_c(s_{\rm max} - s) \delta(s - s_{\rm char}) ds \end{aligned} \tag{16}$$

Integration of Eq. (16) gives

$$\frac{\alpha V \Gamma_1}{\beta \frac{\rho_i}{\rho_a} \frac{\pi}{2}} \frac{1+s_{\max}}{s_{\max}} e^{\frac{2}{\lambda s_{\max}}} = N_{\text{het}}(s_{\max}) D_c(\Delta s_{char}) \quad (17)$$

where $\Delta s_{\text{char}}=s_{\max}-s_{\text{char}}$. Comparing Eqs. (15) and (17) gives,

$$[D_c \otimes n_s](s_{\max}) = N_{\text{het}}(s_{\max}) D_c(\Delta s_{\text{char}}) \quad (18)$$

Equation (18) shows that the terms describing nucleation and growth during the evolution of an ice crystal population can be separated, or, the nucleation spectrum can be determined independently of the dynamics of the parcel ascent. The same conclusion can be obtained by applying Eq. (A5) to Eq. (14), e.g.,

$$\int_0^{s_{\max}} \left[D_c^2 \frac{dD_c}{dt} \otimes n_s \right](s)\, ds = \left[\int_0^{s_{\max}} n_s(s) ds \right] \left[\int_0^{s_{\max}} D_c^2 \frac{dD_c}{dt}\, ds \right] = N_{\text{het}}(s_{\max}) \left[\int_0^{s_{\max}} D_c^2 \frac{dD_c}{dt}\, ds \right] \quad (19)$$

which shows that nucleation and growth can be decoupled independently of the form of $D_c^2 \frac{dD_c}{dt}$.

Equation (18) is a version of the mean value theorem, and physically means that the rate of change of surface area of a polydisperse ice crystal population can be described using the monodisperse approximation, provided that a suitable s_{char} is defined. Equation (18) is a Volterra equation of the first kind and can be solved analytically or numerically (e.g., Linz, 1985). For this, the functional form of $n_s(s_i)$ needs to be known in advance. To keep the parameterization as general as possible, an approximate solution is used instead. $D_c(\Delta s_{\text{char}})$ is expected to be of the order of the largest ice crystals in the population (since they dominate the ice crystal population surface area). As these crystals grow slowly, their size is to first order a linear function of $\Delta s=s_{\max}-s_i$ (Barahona and Nenes, 2009). Therefore, $D_c(\Delta s)$ and $D_c(\Delta s_{\text{char}})$ are related by

$$D_c(\Delta s) \approx D_c(\Delta s_{\text{char}}) \frac{\Delta s}{\Delta s_{\text{char}}} \quad (20)$$

Substituting Eq. (20) into Eq. (18), we obtain,

$$[n_s \otimes \Delta s](s_{\max}) = N_{\text{het}}(s_{\max}) \Delta s_{\text{char}} \quad (21)$$

which after taking the derivative with respect to $s_{\max}$ gives (i.e., Eq. A6),

$$\int_0^{s_{\max}} n_s(s) ds = n_s(s_{\max}) \Delta s_{\text{char}} \quad (22)$$

Application of Eq. (1) to Eq. (22), and rearranging, gives,

$$\Delta s_{\text{char}} = \frac{N_{\text{het}}(s_{\max})}{n_s(s_{\max})} \quad (23)$$

If $s_{\max}$ is large enough, all IN are frozen and $n_s(s_{\max}) \to 0$; this can lead to numerical instability as Δs_{char} becomes very large. However, a large Δs_{char} also implies that a significant fraction of crystals freeze during the early stages of the parcel ascent so that, $s_{\text{char}} \to 0$; hence, $\Delta s_{\text{char}} \to s_{\max}$ and $s_{\max}$ is the upper limit for Δs_{char}. With this, Eq. (23) becomes,

$$\Delta s_{\text{char}} = \min \left(\frac{N_{\text{het}}(s_{\max})}{n_s(s_{\max})}, s_{\max} \right) \quad (24)$$

$D_c(\Delta s_{\text{char}})$ is calculated considering the growth of a monodisperse population with freezing threshold s_{char} (Barahona and Nenes, 2009),

$$D_c(\Delta s_{\text{char}}) = \sqrt{\frac{2\Delta s^*_{\text{char}}}{\alpha V \Gamma_1}} \quad (25)$$

with $\Delta s^*_{\text{char}} = \frac{\Delta s_{\text{char}} \left[\frac{4}{3} \Delta s_{\text{char}} + 2(s_{\max} - \Delta s_{\text{char}}) \right]}{(1+s_{\max}-\Delta s_{\text{char}})}$

Final form for pure heterogeneous freezing

$N_{\text{het}}(s_{\max})$ is calculated from combination of Eqs. (17) and (25),

$$\frac{N_{\text{het}}(s_{\max})}{N^*} = \frac{1}{\sqrt{\Delta s^*_{\text{char}}}} \frac{(1+s_{\max})}{s_{\max}} e^{\frac{2}{\lambda s_{\max}}} \quad (26)$$

with $N^* = \sqrt{2} (\alpha V \Gamma_1)^{3/2} \left(\beta \frac{\pi}{2} \frac{\rho_i}{\rho_a} \right)^{-1}$. Equation (26) is the solution of the s_i balance (Eq. 14) for pure heterogeneous freezing and shows that $N_{\text{het}}(s_{\max})$ depends only on $s_{\max}$, N^*, λ, and Δs_{char}. N^* has dimensions of number concentration and represents the ratio of the rate of increase in s_i from expansion cooling to the rate of increase in the surface area of the crystal population. Δs_{char} is related to the steepness of $n_s(s_i)$ about $s_{\max}$; a value of $\Delta s_{\text{char}} \to 0$ implies that most of the crystals freeze at s_i close to $s_{\max}$. λ accounts for non-continuum effects; if the crystal concentration is low ($\sim$less than 0.01 cm^{-3}) and $\Delta s_{\text{char}} \to s_{\max}$, size effects on $N_{\text{het}}(s_{\max})$ can usually be neglected. Equation (26) is solved along with an expression for $N_{\text{het}}(s_{\max})$ to find $s_{\max}$ (Sect. 3.4, Fig. 2).

3.3 Competition between homogeneous and heterogeneous freezing

At T below 235 K, ice clouds form primarily from homogeneous freezing (e.g., Heymsfield and Sabin, 1989; DeMott et al., 2003a; Barahona and Nenes, 2009). If a significant concentration of IN is present, freezing of IN prior to the onset of homogeneous nucleation may inhibit droplet freezing (Gierens, 2003; Barahona and Nenes, 2009). Equations (7) to (9) can be readily extended to account for this, for which a generalized nucleation spectrum is defined that includes contribution from homogeneous freezing of droplets. This is simplified if taken into account that homogeneous nucleation rates are very high, and, the nucleation spectrum is close to being a delta function about $s_i=s_{\text{hom}}$. Furthermore, since the

number concentration of supercooled liquid droplets available for freezing is much greater than the concentration of IN (i.e., $N_o \gg N_{\rm het}$), $s_{\rm max}$ is reached soon after homogeneous freezing is triggered ($s_{\rm max} \approx s_{\rm hom}$) (Kärcher and Lohmann, 2002a; Barahona and Nenes, 2008). IN freezing thresholds are generally lower than $s_{\rm hom}$; homogeneous freezing can always be considered the last freezing step during ice cloud formation.

As the growth of previously frozen crystals reduces the rate of increase of s_i, (i.e., $\left.\frac{ds_i}{dt}\right|_{s_{\rm hom}}$), the presence of IN tends to reduce the probability of homogeneous freezing and the ice crystal concentration (compared to a pure homogeneous freezing event). The droplet freezing fraction, f_c, in the presence of IN is proportional to the decrease in $\left.\frac{ds_i}{dt}\right|_{s_{\rm hom}}$ (Barahona and Nenes, 2009) from the presence of IN, i.e.,

$$f_c = f_{c,\rm hom} \left(\frac{\left.\frac{ds_i}{dt}\right|_{s_{\rm hom}}}{\alpha V (s_{\rm hom}+1)} \right)^{3/2} \quad (27)$$

where $\alpha V(s_{\rm hom}+1)$ is an approximation to $\left.\frac{ds_i}{dt}\right|_{s_{\rm hom}}$ when IN are not present, and, $f_{c,\rm hom}$ is the droplet freezing fraction under pure homogeneous conditions, given by Barahona and Nenes (2008). Although Eq. (27) is derived for a monodisperse IN population, Eq. (21) suggests that the effect of the polydisperse IN population can be expressed as a monodisperse population, provided that a suitable characteristic freezing threshold, $s_{\rm char}$, is defined. Extending the monodisperse IN population solution (Barahona and Nenes, 2009) to a polydisperse aerosol gives,

$$\frac{\left.\frac{ds_i}{dt}\right|_{s_{\rm hom}}}{\alpha V (s_{\rm hom}+1)} \approx 1 - \left(\frac{N_{het}(s_{\rm hom})}{N_{\rm lim}} \right)^{3/2} \quad (28)$$

where $N_{\rm het}(s_{\rm hom})$ is calculated from the nucleation spectrum function (Sect. 2), and $N_{\rm lim}$ is the limiting IN concentration that completely inhibits homogeneous freezing (Barahona and Nenes, 2009).

If $N_{\rm het}(s_{\rm hom})$ is such that $s_{\rm max}=s_{\rm hom}$, then all IN concentrations greater than $N_{\rm het}(s_{\rm hom})$ would result in $s_{\rm max}<s_{\rm hom}$ and prevent homogeneous freezing (i.e., heterogeneous freezing would be the only mechanism forming crystals). Conversely, if the IN concentration is lower than $N_{\rm het}(s_{\rm hom})$ and $s_{\rm max}>s_{\rm hom}$, homogeneous freezing is active. Thus, $N_{\rm lim}$ must be equal to $N_{\rm het}(s_{\rm hom})$ at $s_{\rm max}=s_{\rm hom}$, and is obtained by substituting $s_{\rm max}=s_{\rm hom}$ into Eq. (26), i.e.,

$$\frac{N_{\rm lim}}{N^*} = \frac{1}{\sqrt{\left.\Delta s^*_{\rm char}\right|_{s_{\rm hom}}}} \frac{(1+s_{\rm hom})}{s_{\rm hom}} e^{\frac{2}{\lambda\, s_{\rm hom}}} \quad (29)$$

For very low $N_{\rm het}$, Eq. (27) approaches the pure homogeneous freezing limit as the effect of IN is negligible; homogeneous freezing is prevented for $N_{\rm het}(s_{\rm hom}) \geq N_{\rm lim}$ and $f_c \leq 0$. Thus, combination of Eqs. (26) and (27) provides the total crystal concentration, N_c, from the combined effects of homogeneous and heterogeneous freezing (Barahona and Nenes, 2009),

$$N_c = \begin{cases} N_o e^{-f_c}(1-e^{-f_c}) + N_{\rm het}(s_{\rm hom}) \\ f_c > 0 \text{ and } T < 235\,\text{K} \\ N_{\rm het}(s_{\rm max}) \\ f_c \leq 0 \text{ or } T > 235\,\text{K} \end{cases} \quad (30)$$

Equation (30) accounts for the fact that homogeneous freezing is not probable for $T>235$ K (e.g., Pruppacher and Klett, 1997) and is applicable only for cases which the cloud remains subsaturated with respect to liquid water (i.e., ice cloud regime).

3.4 Implementation of the parameterization

The generalized parameterization presented in this study is fairly simple to apply and outlined in Fig. 1. Inputs to the parameterization are cloud formation conditions (i.e., p, T, V), liquid droplet and IN aerosol number concentration (i.e., $N_o, N_{\rm dust}, N_{\rm soot}$). Additional inputs (i.e., $s_{h,j}, \theta_j$) may be required depending on the expression used for the nucleation spectrum, $N_{\rm het}(s_i)$. If $T<235$ K, the procedure is to calculate $N_{\rm het}(s_{\rm hom})$, $N_{\rm lim}$ (Eq. 29) and then f_c (Eqs. 27 and 28). If $f_c>0$, then N_c is given by the application of Eq. (30) with $f_{c,\rm hom}$ from Barahona and Nenes (2008). If $f_c \leq 0$ or $T>235$ K, heterogeneous freezing is the only mechanism active, and $N_c=N_{\rm het}(s_{\rm max})$, obtained by numerically solving Eq. (26). Alternatively, precalculated lookup tables or approximate explicit solutions to Eq. (26) can be used to avoid iterative solutions.

4 Evaluation and discussion

The parameterization is tested for all the nucleation spectra presented in Table 1. Only dust and black carbon aerosol is considered, as the contribution of organic carbon to the IN population is sixfold lower than that of black carbon (Phillips et al., 2008). The total surface area of each aerosol population is scaled to the base size distributions of Phillips et al. (2008). For the CNT spectrum a simple linear relation is employed to diagnose $e_{f,j}$, being about 0.05 for dust and soot aerosol particles at $s_i=s_h$ (Pruppacher and Klett, 1997) and decreasing linearly for $s_i<s_h$ (Table 1). Freezing thresholds were set to $s_{h,\rm dust}=0.2$ (Kanji et al., 2008) and $s_{h,\rm soot}=0.3$ (Möhler et al., 2005); $\theta_{\rm dust}$ was set to 16° ($m_{\rm dust}=0.96$) and $\theta_{\rm soot}$ to 40° ($m_{\rm soot}=0.76$) (Chen et al., 2008). $k_{\rm hom}$ is calculated based on Koop et al. (2000) using the fitting of Barahona and Nenes (2008, 2009); $s_{\rm hom}$ is obtained from the analytical fit of Ren and Mackenzie (2005).

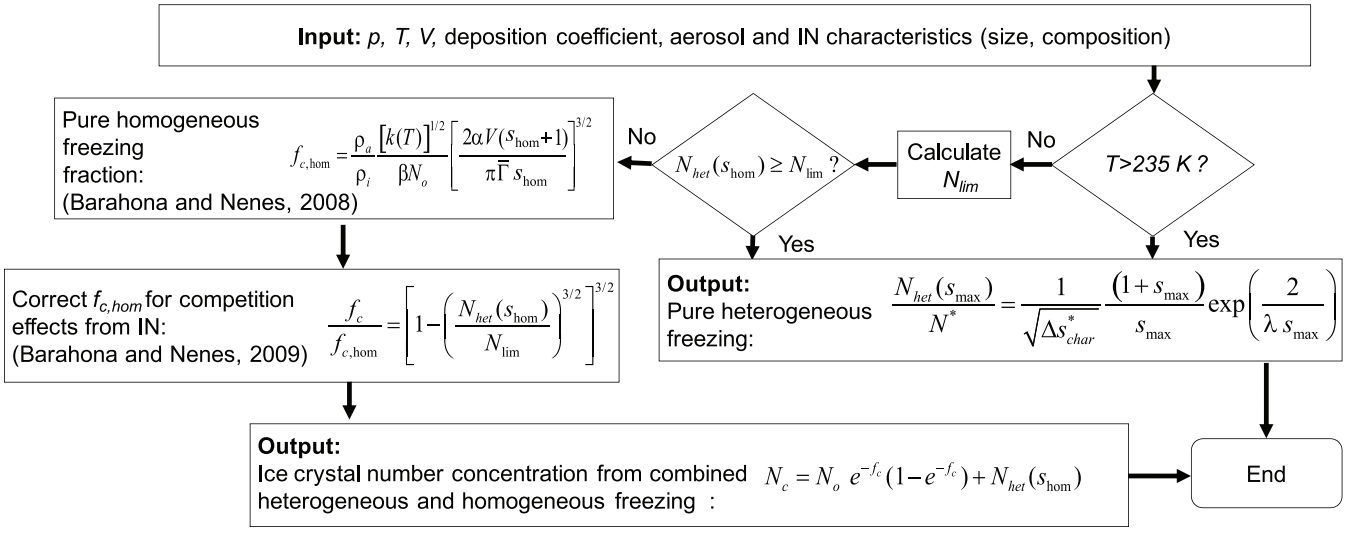

Fig. 1. Parameterization algorithm.

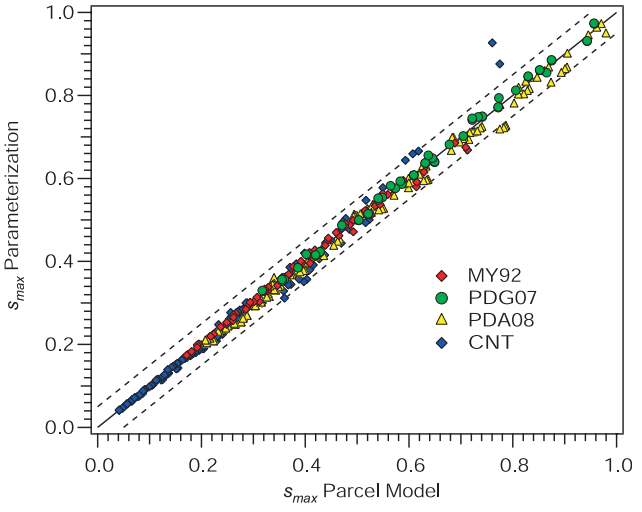

Fig. 2. Comparison between $s_{\max}$ predicted by parameterization and parcel model for conditions of pure heterogeneous freezing. Dashed lines represent ±5% difference.

Table 2. Cloud formation conditions and aerosol characteristic used in the parameterization evaluation.

Property	Values
T_o (K)	205–250
V (m s^{-1})	0.04–2
α_d	0.1, 1.0
$\sigma_{g,\mathrm{dry}}$	2.3
N_o (cm^{-3})	200
$D_{g,\mathrm{dry}}$ (nm)	40
N_{dust} (cm^{-3})	0.05–5
N_{soot} (cm^{-3})	0.05–5
θ_{dust}	16°
θ_{soot}	40°
$s_{h,\mathrm{dust}}$	0.2
$s_{h,\mathrm{soot}}$	0.3

4.1 Comparison against parcel model results

The parameterization was compared against the numerical solution of Eqs. (7) to (9) using the model of Barahona and Nenes (2008, 2009), for all nucleation spectra of Table 1, and conditions of Table 2 (about 1200 simulations overall). To independently test the accuracy of Eqs. (26) and (30), simulations were made under conditions of pure heterogeneous and combined homogeneous-heterogeneous freezing. Calculated N_c ranged from 10^{-4} to 10^2 cm^{-3}; $s_{\max}$ ranged (in absolute units) from 0.05 to 1 for pure heterogeneous freezing (i.e., homogeneous freezing deactivated) and from 0.05 to 0.6 for combined homogeneous-heterogeneous freezing, which covers the expected range of conditions encountered in a GCM simulation.

Figure 2 shows $s_{\max}$ (calculated solving Eq. 26) vs. the parcel model results for conditions of pure heterogeneous freezing. The statistical analysis of the comparison is shown in Table 3 for all nucleation spectra of Table 1 and conditions of Table 2. The overall error with respect to parcel model results is $-1.68\pm3.42\%$, which is remarkably low, given the complexity of Eqs. (7) to (9), and the diversity of $N_{\mathrm{het}}(s_i)$ expressions used. Among the nucleation spectra tested, the largest variability was obtained when using PDA08 ($-2.69\pm2.81\%$) and CNT ($-1.56\pm4.14\%$). This results from variations in the form of the $N_{\mathrm{het}}(s_i)$ function; the distribution functions, $n_s(s_i)$, for MY92 and PDG07 are monotonically increasing and smooth (e.g., Fig. 5) over the

Table 3. Average % relative error (standard deviation) of parameterized N_c and $s_{\max}$ against parcel model simulations. Results are shown for when a) heterogeneous freezing is only active, and, b) homogeneous and heterogeneous nucleation are active. $N_{c,n}$, $N_{c,p}$, are ice crystal concentrations from parcel model and parameterization, respectively; similarly for maximum supersaturation, $s_{\max,n}$, $s_{\max,p}$.

Ice formation mechanism	Pure heterogeneous		Homogeneous and heterogeneous
Spectrum	$\frac{s_{\max,p}-s_{\max,n}}{s_{\max,n}}$	$\frac{N_{c,p}-N_{c,n}}{N_{c,n}}$	$\frac{N_{c,p}-N_{c,n}}{N_{c,n}}$
MY92	0.43(2.29)	1.14(13.3)	2.95(21.2)
PDG07	0.63(1.56)	3.39(7.60)	−3.78(20.7)
PDA08	−2.69(2.81)	−3.26(8.32)	9.64(21.1)
CNT	−0.44(5.56)	−1.56(4.14)	3.26(22.6)
All combined	−1.68(3.42)	−2.08(8.58)	4.72(21.8)

entire s_i range considered. PDA08 and CNT are characterized by abrupt changes in $N_{\rm het}(s_i)$ which produces discontinuities in $n_s(s_i)$. This is evident for the CNT spectrum as the error in the calculation of $s_{\max}$ lowers (−0.44±5.6 %) if only data with $s_{\max}<s_{h,\rm soot}$ is considered. CNT also shows a slight overestimation of $s_{\max}$ at high values caused by the assumption of $s_{h,\rm char}$=0 when $n_s(s_i)$=0, Eq. (24); this however is not a source of uncertainty for $N_{\rm het}$ calculation (Fig. 3) as crystal concentration is constant for $s_{\max}>s_{h,\rm soot}$ (Table 1). Another source of discrepancy (which is however never outside of the ±5% range) is the small change in T (∼4 K), from s_i=0 to s_i=$s_{\max}$ which is larger at high V and causes an slight underestimation of $s_{\max}$ at high values (∼$s_{\max}$>0.7) for the PDG07 and MY92 spectra.

Figure 3 shows that the error in $N_{\rm het}$ calculation is also quite low, −2.0±8.5%, which indicates no biases in the parameterization. The slightly larger error in N_c compared to the error in $s_{\max}$ originates from the sensitivity of $N_{\rm het}(s_{\max})$ to small variations in $s_{\max}$. Figure 3 shows that the larger discrepancy in $s_{\max}$ (Fig. 2) when using the CNT and PDA08 spectra does not translate into a large error in $N_{\rm het}$ which remains low for these cases (∼5%). The largest variability (±13.5%) was found using MY92 and is related to the slight underestimation of $s_{\max}$ at high V ($s_{\max}>0.7$). $\Delta s_{\rm char}$ for MY92 is around 0.07 (whereas for the other spectra of Table 1 it is generally above 0.2) which indicates that most crystals in the MY92 spectrum freeze at s_i close to $s_{\max}$ (Eq. 24); MY92 is therefore most sensitive to the small underestimation in $s_{\max}$ at high V.

When competition between homogeneous and heterogeneous nucleation is considered (Fig. 4), $s_{\max}\approx s_{\rm hom}$, and no explicit dependency of N_c on $s_{\max}$ is considered; this approximation however does not introduce substantial error in the calculation of N_c (Barahona and Nenes, 2008). The overall error in N_c calculation for this case is 4.7±21%. Comparison of Figs. 3 and 4 suggests that most of the error results from the inherent error of the homogeneous nucleation scheme (1±28%, Barahona and Nenes, 2008). Figure 4 shows that the parameterization reproduces the parcel model results from the pure heterogeneous (i.e., $\frac{N_{\rm het}}{N_{\rm lim}}>1$) to the pure homogeneous (i.e., $\frac{N_{\rm het}}{N_{\rm lim}}\rightarrow 0$) freezing limit. The largest discrepancy (−9.6±21%) occurs when the PDA08 spectrum is used, and is related to the complexity of the $N_{\rm het}(s_i)$ function. Larger variations (mostly within a factor of 2) also occur when $N_{\rm het}(s_{\max})\rightarrow N_{\rm lim}$ and are caused by the high sensitivity of N_c to $N_{\rm het}(s_{\max})$ for $\frac{N_{\rm het}}{N_{\rm lim}}\approx 1$ (cf., Barahona and Nenes, 2009, Fig. 3).

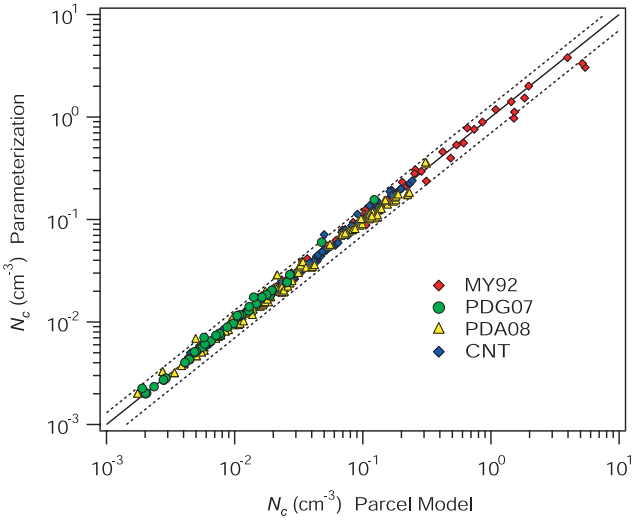

Fig. 3. Comparison between $N_{\rm het}$ from pure heterogeneous freezing predicted by the parameterization and the parcel model for simulation conditions of Table 2 and freezing spectra of Table 1. Dashed lines represent the ±30% difference.

4.2 Comparison against existing schemes

The new parameterization was compared against the schemes of Liu and Penner (2005, LP05) and Kärcher et al. (2006, K06), for all spectra of Table 1 and, for T=206 K, p=22 000 Pa, and, α_d=0.5. Consistent with K06, the maximum number concentration of IN was set to 0.005 cm^{-3}, which for $e_{f,\rm soot}$=0.05 implies $N_{\rm soot}$=0.1 cm^{-3}. Cases with no dust present (i.e., $N_{\rm dust}$=0 and no deposition freezing

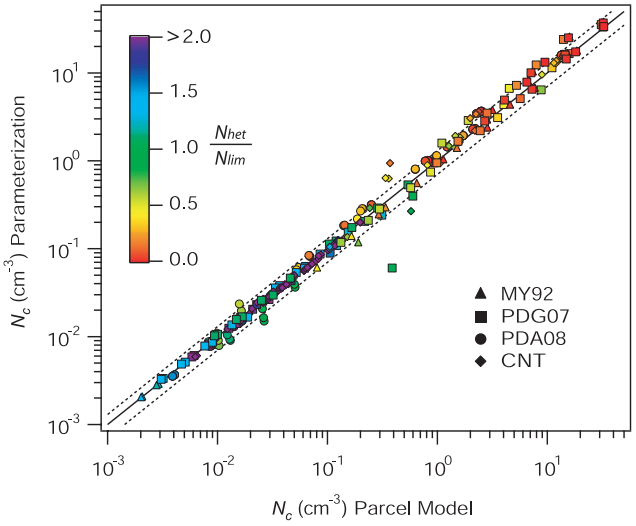

Fig. 4. Comparison between N_c from combined homogeneous and heterogeneous freezing predicted by the parameterization and the parcel model for simulation conditions of Table 2 and freezing spectra of Table 1. Dashed lines represent the ±30% difference. Colors indicate the ratio $\frac{N_{\rm het}}{N_{\rm lim}}$.

in LP05) and with $N_{\rm dust}$=$N_{\rm soot}$ were considered. For the "no-dust" case (Fig. 5, left) K06 and the new parameterization (Eq. 30), using the CNT, MY92, and PDG07 spectra, agree within a factor of two at the pure heterogeneous limit ($\sim V<0.01\,{\rm m\,s^{-1}}$). Homogenous freezing in these cases is triggered (i.e., $N_{\rm lim}>N_{\rm het}$) between 0.03 and 0.07 m s^{-1} except when using MY92, where $V>0.7\,{\rm m\,s^{-1}}$ is needed to allow homogeneous freezing. When using Eq. (30) and PDA08, a much lower $N_{\rm het}$ is predicted over the entire V range considered, and homogeneous freezing is triggered at very low $V\sim0.002\,{\rm m\,s^{-1}}$ (i.e., heterogeneous freezing has a negligible effect on N_c).

LP05 predicts $N_{\rm het}$ about two orders of magnitude higher than the application of Eq. (30) to the PDG07 and CNT spectra. This discrepancy may result from the high $e_{f,{\rm soot}}\sim1$ implied in this parameterization compared to the other freezing spectra considered (which is evident for $V>0.04\,{\rm m\,s^{-1}}$ as $N_{\rm het}\approx N_{\rm soot}$). LP05 also predicts complete inhibition of homogeneous freezing up to $V\sim0.3\,{\rm m\,s^{-1}}$ (Fig. 5, right) which is much larger than the range between 0.03 and 0.07 m s^{-1} found by application of Eq. (30). The discrepancy between LP05 and the other schemes in Fig. 5 is due to differences in the values of $s_{h,{\rm soot}}$ and α_d used in generating LP05. In fact, the results of LP05 can be approximately reproduced by setting $e_{f,{\rm soot}}$=1.0 and $s_{h,{\rm soot}}$=0.1 in the CNT profile and by changing the value of α_d to 0.1, as shown in the CNT(b) curves of Figs. 5 and 6. The lower value of $s_{h,{\rm soot}}$=0.1 required to reproduce LP05, compared to the one used by Liu and Penner (2005), $s_{h,{\rm soot}}$=0.2, results from the smoother freezing pulse in the CNT model as opposed to the step function implied by the model of Liu and Penner (2005).

When similar concentrations of dust and soot are considered (Fig. 5 right), Eq. (30) with PDA08 come much closer to simulations using CNT and PDG07. K06 (maintaining $N_{\rm IN}$=0.005 cm^{-3}) still lies within a factor of two from the results obtained with Eq. (30) and the CNT, PDA08, and PDG07 spectra. By including dust, the onset of homogeneous nucleation is triggered at slightly higher V, compared to the case with no dust (CNT). For PDA08, the change is more pronounced, indicating that the maximum $e_{f,{\rm dust}}$ implied by PDA08 is substantially larger than $e_{f,{\rm soot}}$ for the same spectrum, i.e., most of the crystals in this case come from freezing of dust. At the pure homogeneous freezing limit ($V\sim1\,{\rm m\,s^{-1}}$), IN effects on N_c are unimportant, and, N_c for all spectra agree well with K06 (Barahona and Nenes, 2008). At this limit, LP05 predicts a twofold higher N_c due to the different set of parameters used in its development (Liu and Penner, 2005). The discrepancy between LP05 and the CNT profile can be reconciled by setting $e_{f,{\rm soot}}$=1, $s_{h,{\rm soot}}$=0.1, and α_d=0.1.

A comparison of predicted $s_{\rm max}$ between the new parameterization and LP05 was also carried out. The curves of Fig. 6 can be used to explain the profiles of Fig. 5, as homogeneous freezing is prevented if $s_{\rm max}<s_{\rm hom}$ (Gierens, 2003; Barahona and Nenes, 2009). When dust is not included, $s_{\rm max}$ calculated using PDA08 approaches $s_{\rm hom}$ at very low V, therefore allowing homogeneous nucleation to take place in almost the entire range of V considered (not shown). When dust is included, $s_{\rm max}$ calculated using Eq. (30) and the PDG07, PDA08 and CNT spectra approaches $s_{\rm hom}$ for V between 0.02 and 0.06 m s^{-1}. When using MY92, $s_{\rm max}$ is below $s_{\rm hom}$ for almost the entire range of V considered, and, explains why homogeneous freezing is prevented for most values of V. LP05 predicts a very different $s_{\rm max}$ profile , being constant ($s_{\rm max}\sim0.2$) at low V, then a steep increase in $s_{\rm max}$ around $V\sim0.1\,{\rm m\,s^{-1}}$ which reaches $s_{\rm hom}$ at $V\sim0.3\,{\rm m\,s^{-1}}$. In this case, setting $e_{f,{\rm soot}}$=1, $s_{h,{\rm soot}}$=0.1, and α_d=0.1 reduces the discrepancy between LP05 and CNT (curve CNT (b)) for $s_{\rm max}\sim s_{\rm hom}$ and $V\sim0.2$–$0.3\,{\rm m\,s^{-1}}$. The two schemes however still diverge at $V<0.1\,{\rm m\,s^{-1}}$.

5 Summary and conclusions

We present an ice cloud formation parameterization that calculates N_c and $s_{\rm max}$ explicitly considering the competition between homogeneous and heterogeneous freezing from a polydisperse (in size and composition) aerosol population. Heterogeneous freezing is accounted for by using a nucleation spectrum that could have any functional form. Analytical solution of the parcel model equations was accomplished by reformulating the supersaturation balance and by introducing the concepts of characteristic freezing threshold and characteristic size of a polydisperse ice crystal population. The approach presented here successfully decouples the nucleation and growth factors in the solution of the

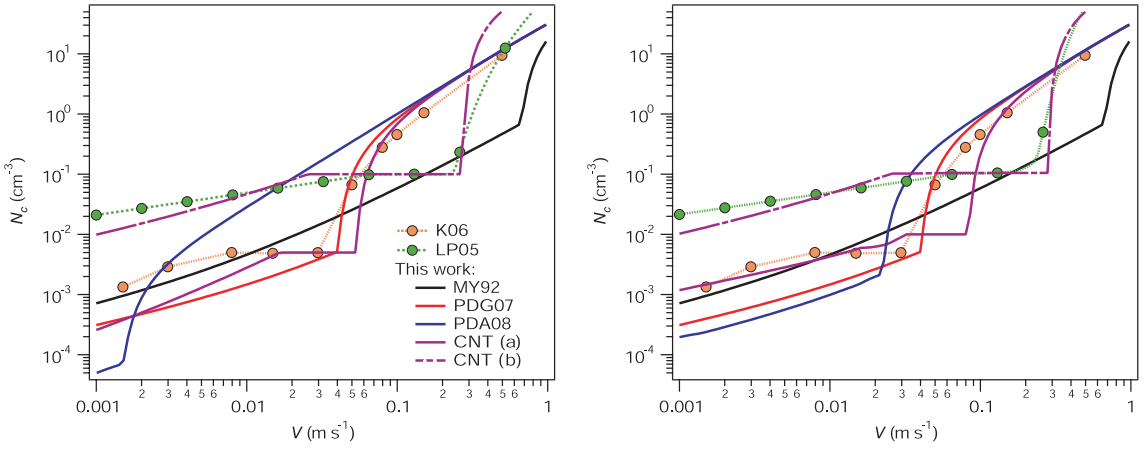

Fig. 5. N_c vs. V calculated using the new parameterization for all freezing spectra of Table 1. Also shown are results taken from Kärcher et al. (2006, K06) for $N_{IN}=5\times10^{-3}$ cm^{-3} and, the parameterization of Liu and Penner (2005). Conditions considered were T_o=210 K (T=206 K), p=22 000 Pa, α_d=0.5. Left panel: N_{soot}=0.1 cm^{-3}, N_{dust}=0 cm^{-3} and no deposition freezing considered in LP05. Right panel: N_{soot}=0.1 cm^{-3}, N_{dust}=0.1 cm^{-3} and deposition freezing considered in LP05. For CNT(a) runs were made as presented in Tables 1 and 2 while for CNT(b) conditions were changed to $s_{h,soot}$=0.1, $e_{f,soot}$=1.0, and α_d=0.1.

supersaturation balance, and together with the work of Barahona and Nenes (2008, 2009), provides a comprehensive parameterization for ice cloud formation. The parameterization was tested with a diverse set of published IN spectra (Table 1), which includes a formulation introduced here derived from classical nucleation theory.

When evaluated over a wide set of conditions and IN nucleation spectra, the parameterization reproduced detailed numerical parcel model results to −1.6±3.4% and −2.0±8.5%, for the calculation of s_{max} and N_{het} from pure heterogeneous freezing, respectively, and 4.7±21% for the calculation of N_c from combined homogeneous and heterogeneous freezing. Comparison against other formulations over a limited set of conditions showed that changes in the freezing efficiency of each IN population (i.e., dust and soot) is the main factor determining the effect of heterogeneous freezing on the total ice crystal concentration, N_c. The variability of N_c shown in Fig. 6 is however much lower than reported by Phillips et al. (2008), who compared several nucleation spectra at fixed s_i; this emphasizes the importance of using a proper dynamic framework in comparing nucleation spectra.

During the development of the parameterization (Sect. 3) it was implicitly assumed that the cloudy parcel is initially devoid of ice crystals. If cirrus persist beyond the time step of the host model, then the effect of preexisting ice crystals should be accounted for in the parameterization by including an additional water vapor depletion term at the left hand side of Eq. (14). This effect however may be small as crystals with large sizes tend to fall out of the nucleation zone (i.e., the zone with highest supersaturation in the cloud) during the evolution of the cirrus cloud (Spichtinger and Gierens, 2009). If the heterogeneously nucleated ice crystals fall out however

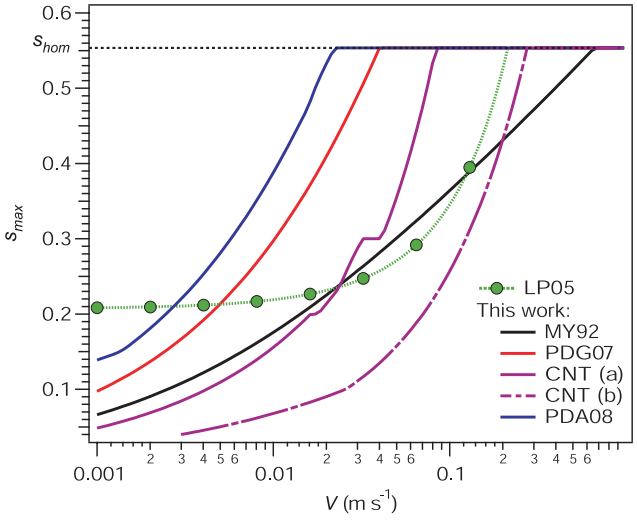

Fig. 6. s_{max} vs. V calculated using the parameterization of Liu and Penner (2005) and the new parameterization for all freezing spectra of Table 1. Conditions considered are similar to Fig. 5 and $N_{soot}=N_{dust}$=0.1 cm^{-3}. For CNT(b) $s_{h,soot}$=0.1, $e_{f,soot}$=1.0, and α_d=0.1.

from the nucleation zone before s_{max} is reached, the effect of IN on homogeneous nucleation may be reduced. Theoretical studies (Kay et al., 2006; Spichtinger and Gierens, 2009) suggest that deposition effects may be significant at low V (<0.05 m s^{-1}) and low N_{het} (<0.01 cm^{-3}). Deposition effects can be included in Eq. (14) by adding a "fallout" term (Kay et al., 2006) to the supersaturation balance, Eq. (7), and is the subject of a companion study.

The parameterization presented in this work is suitable for large-scale atmospheric models that cannot resolve ice supersaturation at the scale of cloud formation (∼50 m (Pruppacher and Klett, 1997)). It is computationally efficient and analytically unravels the dependency of ice crystal concentration on cloud formation conditions (T,p,V), deposition coefficient, the size and composition of the droplet population, and insoluble aerosol (i.e., IN) concentrations. It provides a framework in which new ice nucleation data can easily be incorporated in aerosol-cloud interaction studies.

Appendix A

The convolution product

Let f_1 and f_2 be two locally integrable functions over the real axis, then the function

$$(f_1 * f_2)(x) = \int_0^\infty f_1(v) f_2(x-v) dv \tag{A1}$$

is called the convolution product of f_1 and f_2 (Kecs, 1982). The half-convolution product (or convolution of the half-axis) is defined for $x \geq 0$ as

$$(f_1 \otimes f_2)(x) = \int_0^x f_1(v) f_2(x-v) dv \tag{A2}$$

and related to the convolution product by

$$(f_1 \otimes f_2)(x) = [\mathrm{H}(f_1) * \mathrm{H}(f_2)](x) \tag{A3}$$

where H is the Heaviside function,

$$\mathrm{H}(v) = \begin{cases} 0, & v < 0 \\ 1, & v \geq 0 \end{cases} \tag{A4}$$

The convolution product is commutative and distributive; its integral is given by

$$\int (f_1 * f_2)\, dx = \int f_1(u) du \int f_2(v) dv \tag{A5}$$

its derivative is expressed as

$$\frac{d}{dx}(f_1 * f_2)(x) = \left(\frac{df_1}{dx} * f_2\right)(x) = \left(f_1 * \frac{df_2}{dx}\right)(x) \tag{A6}$$

Appendix B

Analytical correction for non-continuum effects

The lower limit for the size of an ice crystal ice crystal that freezes at supersaturation $s_o'=0$ during the parcel ascent (Ren and Mackenzie, 2005; Barahona and Nenes, 2008), obtained assuming $\left.\frac{ds_i}{dt}\right|_{s_{\max}} \approx \alpha V (s_{\max}+1)$, is given by

$$D_c(\Delta s, \alpha_d) = -\frac{\Gamma_2}{\Gamma_1} + \sqrt{\left(\frac{\Gamma_2}{\Gamma_1}\right)^2 + \frac{\Delta s^2}{\alpha V \Gamma_1}} \tag{B1}$$

where $\Delta s = s_{\max} - s_o'$ and it was assumed that $\Delta s - \ln\left(\frac{s_{\max}+1}{s_o'+1}\right) \approx \frac{1}{2}\Delta s^2$. D_c depends on α_d as $\Gamma_2 \propto \frac{1}{\alpha_d}$. Equation (B1) provides a lower limit for D_c and can be used to develop a conservative (i.e., where mass transfer limitations to crystal growth are most significant) correction for non-continuum mass transfer effects. Equation (B1) can be rewritten as

$$D_c(\Delta s, \alpha_d) = \gamma\left[\sqrt{1+(\lambda\Delta s)^2} - 1\right] \tag{B2}$$

where $\gamma = \frac{\Gamma_2}{\Gamma_1}$, $\lambda = \sqrt{\frac{1}{\alpha V \Gamma_1 \gamma^2}}$. After substituting Eq. (B2) into Eq. (9) and rearranging, the volumetric rate of change of an ice crystal at $s_{\max}$, i.e., $\frac{\pi}{2} D_c^2 \frac{dD_c}{dt} = \frac{\pi}{2} \frac{s_{\max} D_c^2}{\Gamma_1 D_c + \Gamma_2}$, can be written in the form

$$\frac{\pi}{2} D_c^2 \frac{dD_c}{dt} = \frac{\pi}{2} \frac{s_{\max}}{\Gamma_1} \frac{\gamma\left(1-\sqrt{1+(\lambda\Delta s)^2}\right)^2}{\sqrt{1+(\lambda\Delta s)^2}} \tag{B3}$$

Multiplying an dividing the right hand side of Eq. (B3) by $\lambda\Delta s$ and rearranging gives,

$$\frac{\pi}{2} D_c^2 \frac{dD_c}{dt} = \left[\frac{\pi}{2} \frac{s_{\max}\gamma\lambda\Delta s}{\Gamma_1}\right]\left[\frac{\left(1-\sqrt{1+(\lambda\Delta s)^2}\right)^2}{\lambda\Delta s\sqrt{1+(\lambda\Delta s)^2}}\right] \tag{B4}$$

It can be recognized that the first term in brackets in Eq. (B4) is obtained from $\frac{\pi}{2} D_c^2 \frac{dD_c}{dt} = \frac{\pi}{2} \frac{s_{\max} D_c^2}{\Gamma_1 D_c + \Gamma_2}$, taking into account Eq. (B1), when $\Gamma_1 \gg \Gamma_2$, i.e., when non-continuum effects on mass transfer can be neglected (cf. Barahona and Nenes, 2008, Sect. 3.3). Thus, the second term in brackets in Eq. (B4) corresponds to a correction factor to $\frac{\pi}{2} D_c^2 \frac{dD_c}{dt}$ for non-continuum mass transfer effects, which only depends on the product $\lambda\Delta s$. Equation (11) suggests that $\lambda s_{\max}$ is a characteristic value for $\lambda\Delta s$, therefore Eq. (B4) can be rewritten as

$$\frac{\pi}{2} D_c^2 \frac{dD_c}{dt} \approx \frac{\pi}{2} \frac{s_{\max} D_c(\Delta s)}{\Gamma_1} \frac{\left(1-\sqrt{1+\lambda^2 s_{\max}^2}\right)^2}{\lambda s_{\max}\sqrt{1+\lambda^2 s_{\max}^2}} \tag{B5}$$

For $s_{\max} > 0.05$, Eq. (B5) can be approximated by

$$\frac{\pi}{2} D_c^2 \frac{dD_c}{dt} \approx \frac{\pi}{2} \frac{s_{\max} D_c(\Delta s)}{\Gamma_1} e^{-\frac{2}{\lambda s_{\max}}} \tag{B6}$$

Appendix C

List of symbols and abbreviations

α	$\frac{g\Delta H_s M_w}{c_p RT^2} - \frac{a_g M_a}{RT}$
α_d	Deposition coefficient of water vapor to ice
a_g	Acceleration of gravity
β	$\frac{M_a p}{M_w p_i^o} - \frac{\Delta H_s^2 M_w}{c_p RT^2}$
γ	$\frac{\Gamma_2}{\Gamma_1}$
c_p	Specific heat capacity of air
D_c	Volume sphere-equivalent diameter of an ice particle
ΔH_s	Enthalpy of sublimation of water
$D_{\rm IN}$	Volume sphere-equivalent diameter of an IN
Δs	$s_{\max} - s'_o$
$\Delta s_{\rm char}$	$s_{\max} - s_{\rm char}$
$\Delta s^*_{\rm char}$	Growth integral, defined by Eq. (25)
D_v	Water vapor mass transfer coefficient
$e_{f,j}$	Maximum freezing efficiency of the j-th IN species
f_c,hom, f_c	Fraction of frozen particles at s_{hom} with and without IN present, respectively.
$f_{h,j}$	Shape factor of the j-th IN species
Γ_1	$\frac{\rho_i RT}{4p_i^o D_v M_w} + \frac{\Delta H_s \rho_i}{4k_a T}\left(\frac{\Delta H_s M_w}{RT} - 1\right)$
Γ_2	$\frac{\rho_i RT}{2p_i^o M_w}\sqrt{\frac{2\pi M_w}{RT}}\frac{1}{\alpha_d}$
H	Heaviside function
$J(s_i)$, J	Nucleation rate coefficient at s_i
$J_{\rm hom}(s_{\rm hom})$	Homogenous nucleation rate coefficient at $s_{\rm hom}$
$J_{h,j}(s_{h,j})$	Heterogeneous nucleation rate coefficient at the freezing threshold of the j-th IN population
$k(T)$	Freezing parameter defined by Eq. (2)
k_a	Thermal conductivity of air
$k_{\rm hom}$	Homogeneous freezing parameter, $\ln \frac{J_{\rm hom}(s_{\rm hom})}{J_{\rm hom}(s_i)}(s_{\rm hom} - s_i)^{-1}$
λ	$\sqrt{\frac{1}{\alpha V \Gamma_1 \gamma^2}}$
$m_{1\ldots nx}$	Multidimensional variable that symbolizes the mass fraction of the *nx* chemical species present in an aerosol population
m_j	Wettability parameter of the j-th IN species, $\cos(\theta_j)$
M_w, M_a	Molar masses of water and air, respectively
N^*	$\sqrt{2}\,(\alpha V\,\Gamma_1)^{3/2}\left(\beta\frac{\pi}{2}\frac{\rho_i}{\rho_a}\right)^{-1}$
$N_{a,j}$	Number concentration of the j-th insoluble aerosol species
N_c	Total ice crystal number concentration
$n_c(D_c, D_{\rm IN}, m, t)$	Number distribution of the ice crystals
$N_{\rm dust}$	Dust number concentration
$N_{\rm soot}$	Soot number concentration
$N_{\rm het}$	Ice crystals number concentration from heterogeneous freezing
$N_{\rm het}(s_i)$	Cumulative heterogeneous nucleation spectrum
$N_{\rm hom}(s_i)$	Cumulative homogeneous nucleation spectrum
$N_{\rm IN}$	Maximum IN number concentration
$N_{\rm lim}$	Limiting $N_{\rm IN}$ that would prevent homogeneous nucleation
N_o	Number concentration of the supercooled liquid droplet population
$n_s(s_i)$	Heterogeneous nucleation spectrum
nsp	Number of externally mixed IN populations
nx	Number of chemical species present in the aerosol population
p	Ambient pressure
P_f	Freezing probability
p_i^o	Ice saturation vapor pressure
R	Universal gas constant
ρ_i, ρ_a	Ice and air densities, respectively
$s_{h,j}$	Freezing threshold of the j-th IN species
$s_{\rm char}$	Characteristic freezing threshold of the heterogeneous IN population
$s_{\rm hom}$	Homogeneous freezing threshold
s_i	Water vapor supersaturation ratio with respect to ice
$s_{\max}$	Maximum ice supersaturation ratio
s'_o	Freezing threshold of an IN
T	Temperature
T_o	Initial temperature of the cloudy parcel
t	Time

θ_j	Contact angle between the j-th IN species surface and water
V	Updraft velocity
$\bar{v}_o$	Mean volume of the droplet population
w_i	Ice mass mixing ratio
X	Domain of integration in Eq. (6)
$\bar{\Omega}_j$	Mean surface area of the j-th insoluble aerosol population

Acknowledgements. This study was supported by NASA MAP, NASA ACMAP and a NASA New Investigator Award.

Edited by: P. Spichtinger

References

Abbatt, J. P. D., Benz, S., Cziczo, D. J., Kanji, Z., and Möhler, O.: Solid ammonium sulfate as ice nuclei: a pathway for cirrus cloud formation, Science, 313, 1770–1773, 2006.

Archuleta, C. M., DeMott, P. J., and Kreidenweis, S. M.: Ice nucleation by surrogates for atmospheric mineral dust and mineral dust/sulfate particles at cirrus temperatures, Atmos. Chem. Phys., 5, 2617–2634, 2005, http://www.atmos-chem-phys.net/5/2617/2005/.

Baker, M. B. and Peter, T.: Small-scale cloud processes and climate, Nature, 451, 299–300, 2008.

Barahona, D. and Nenes, A.: Parameterization of cirrus formation in large scale models: Homogenous nucleation, J. Geophys. Res., 113, D11211, doi:11210.11029/12007JD009355, 2008.

Barahona, D. and Nenes, A.: Parameterizing the competition between homogeneous and heterogeneous freezing in cirrus cloud formation – monodisperse ice nuclei, Atmos. Chem. Phys., 9, 369–381, 2009, http://www.atmos-chem-phys.net/9/369/2009/.

Chen, J.-P., Hazra, A., and Levin, Z.: Parameterizing ice nucleation rates using contact angle and activation energy derived from laboratory data, Atmos. Chem. Phys., 8, 7431–7449, 2008, http://www.atmos-chem-phys.net/8/7431/2008/.

Chen, Y., DeMott, P. J., Kreidenweis, S. M., Rogers, D. C., and Sherman, D. E.: Ice formation by sulfate and sulfuric acid aerosol particles under upper-tropospheric conditions, J. Atmos. Sci., 57, 3752–3766, 2000.

Cziczo, D. J. and Abbatt, J. P. D.: Ice nucleation in NH_4HSO_4, NH_4NO_3, and H_2SO_4 aqueous particles: Implications for cirrus formation, Geophys. Res. Lett., 28, 963–966, 2001.

DeMott, P. J., Meyers, M. P., and Cotton, R. W.: Parameterization and impact of ice initiation processes relevant to numerical model simulations of cirrus clouds, J. Atmos. Sci., 51, 77–90, 1994.

DeMott, P. J., Rogers, D. C., and Kreidenweis, S. M.: The susceptibility of ice formation in upper tropospheric clouds to insoluble aerosol components, J. Geophys. Res., 102, 19575–19584, 1997.

DeMott, P. J., Rogers, D. C., Kreidenweis, S. M., Chen, Y., Twohy, C. H., Baumgardner, D. G., Heymsfield, A. J., and Chan, K. R.: The role of heterogeneous freezing nucleation in upper tropospheric clouds: Inferences from SUCCESS, Geophys. Res. Lett., 25, 1387–1390, 1998.

DeMott, P. J., Cziczo, D. J., Prenni, A. J., Murphy, D. M., Kreidenweis, S. M., Thompson, D. S., Borys, R., and Rogers, D. C.: Measurements of the concentration and composition of nuclei for cirrus formation, Proc. Natl. Acad. Sci. USA, 100, 14655–14660, 2003a.

DeMott, P. J., Sassen, K., Poellot, M. R., Baumgardner, D. G., Rogers, D. C., Brooks, S. D., Prenni, A. J., and Kreidenweis, S. M.: African dust aerosols as atmospheric ice nuclei, Geophys. Res. Lett., 30, 1732, doi:1710.1029/2003GL017410, 2003b.

Eastwood, M. L., Cremel, S., Gehrke, C., Girard, E., and Bertram, A. K.: Ice nucleation on mineral dust particles: Onset conditions, nucleation rates and contact angles, J. Geophys. Res., 113, D22203, doi:22210.21029/22008JD10639, 2008.

Eidhammer, T., DeMott, P. J., and Kreidenweis, S. M.: A comparison of heterogeneous ice nucleation parameterizations using a parcel model framework, J. Geophys. Res., 114, doi:10.1029/2008JD011095, 2009.

Field, P. R., Möhler, O., Connolly, P., Krmer, M., Cotton, R., Heymsfield, A. J., Saathoff, H., and Schnaiter, M.: Some ice nucleation characteristics of Asian and Saharan desert dust, Atmos. Chem. Phys., 6, 2991–3006, 2006, http://www.atmos-chem-phys.net/6/2991/2006/.

Fletcher, H. N.: On ice-crystal production by aerosol particles, J. Atmos. Sci., 16, 173–180, 1959.

Fletcher, H. N.: Active sites and ice crystal nucleation, J. Atmos. Sci., 26, 1266–1271, 1969.

Gayet, J. F., Ovarlez, J., Shcherbakov, V., Ström, J., Schumann, U., Minikin, A., Auriol, F., Petzold, A., and Monier, M.: Cirrus cloud microphysical and optical properties at southern and northern midlatitudes during the INCA experiment, J. Geophys. Res., 109, D20206, doi:20210.21029/22004JD004803, 2004.

Gierens, K.: On the transition between heterogeneous and homogeneous freezing, Atmos. Chem. Phys., 3, 437–446, 2003, http://www.atmos-chem-phys.net/3/437/2003/.

Haag, W., Kärcher, B., Schaefers, S., Stetzer, O., Möhler, O., Schurath, U., Krämer, M., and Schiller, C.: Numerical simulations of homogeneous freezing processes in the aerosol chamber AIDA, Atmos. Chem. Phys., 3, 195–210, 2003a, http://www.atmos-chem-phys.net/3/195/2003/.

Haag, W., Kärcher, B., Ström, J., Minikin, A., Lohmann, U., Ovarlez, J., and Stohl, A.: Freezing thresholds and cirrus cloud formation mechanisms inferred from in situ measurements of relative humidity, Atmos. Chem. Phys., 3, 1791–1806, 2003b, http://www.atmos-chem-phys.net/3/1791/2003/.

Hartmann, D. L., Holton, J. R., and Fu, Q.: The heat balance of the tropical tropopause, cirrus, and stratospheric dehydration, Geophys. Res. Lett., 28, 1969–1972, 2001.

Heymsfield, A. J. and Platt, C. M.: A parameterization of the particle size spectrum of ice clouds in terms of the ambient temperature and ice water content, J. Atmos. Sci., 41, 846–855, 1984.

Heymsfield, A. J. and Sabin, R. M.: Cirrus crystal nucleation by homogenous freezing of solution droplets., J. Atmos. Sci., 46, 2252–2264, 1989.

Hung, H., Malinowski, A., and Martin, S. T.: Ice nucleation kinetics of aerosols containing aqueous and solid ammonium sulfate, J. Phys. Chem. A, 106, 293–306, 2002.

Kanji, Z. A., Florea, O., and Abbatt, J. P. D.: ice formation via deposition nucleation on mineral dust and organics: dependence of onset relative humidity on total particulate surface area, Environ.

Res. Lett., 3, doi:10.1088/1748-9326/1083/1082/025004, 2008.

Kärcher, B. and Lohmann, U.: A parameterization of cirrus cloud formation: homogeneous freezing of supercooled aerosols, J. Geophys. Res., 107, 4010, doi:4010.1029/2001JD000470, 2002a.

Kärcher, B. and Lohmann, U.: A parameterization of cirrus cloud formation: homogeneous freezing including effects or aerosol size, J. Geophys. Res., 107, 4698, doi:4610.1029/2001JD001429, 2002b.

Kärcher, B. and Lohmann, U.: A parameterization of cirrus cloud formation: Heterogeneous freezing, J. Geophys. Res., 108, 4402, doi:4410.1029/2002JD003220, 2003.

Kärcher, B., Hendricks, J., and Lohmann, U.: Physically based parameterization of cirrus cloud formation for use in global atmospheric models, J. Geophys. Res., 111, D01205, doi:01210.01029/02005JD006219, 2006.

Kärcher, B., Möhler, O., DeMott, P. J., Pechtl, S., and Yu, F.: Insights into the role of soot aerosols in cirrus cloud formation, Atmos. Chem. Phys., 7, 4203–4227, 2007, http://www.atmos-chem-phys.net/7/4203/2007/.

Kay, J. E., Baker, M. B., and Hegg, D.: Microphysical and dynamical controls on cirrus cloud optical depth distributions, J. Geophys. Res., 111, D24205, doi:24210.21029/22005JD006916, 2006.

Kecs, W.: The convolution product and some applications, Mathematics and its applications, D. Reidel co., Bucharest, Romania, 1982.

Khvorostyanov, V. I. and Curry, J. A.: The theory of ice nucleation by heterogeneous freezing of deliquescent mixed CCN. Part I: critical radius, energy and nucleation rate, J. Atmos. Sci., 61, 2676–2691, 2004.

Khvorostyanov, V. I. and Curry, J. A.: The theory of ice nucleation by heterogeneous freezing of deliquescent mixed CCN. Part II: parcel model simulations, J. Atmos. Sci., 62, 261–285, 2005.

Khvorostyanov, V. I. and Curry, J. A.: Critical humidities of homogeneous and heterogeneous ice nucleation: Inferences from extended classical nucleation theory, J. Geophys. Res., 114, D04207, doi:04210.01029/02008JD011197, 2009.

Koop, T., Luo, B., Tslas, A., and Peter, T.: Water activity as the determinant for homogeneous ice nucleation in aqueous solutions, Nature, 406, 611–614, 2000.

Lau, K. M. and Wu, H. T.: Warm rain processes over tropical oceans and climate implications, Geophys. Res. Lett., 30, 2290, doi:2210.1029/2003GL018567, 2003.

Lin, R., Starr, D., DeMott, P. J., Cotton, R., Sassen, K., Jensen, E. J., Kärcher, B., and Liu, X.: Cirrus parcel model comparison project. Phase 1: The critical components to simulate cirrus initiation explicitly, J. Atmos. Sci., 59, 2305–2328, 2002.

Linz, P.: Analytical and numerical methods for Volterra equations, SIAM studies in applied mathematics, SIAM, Philadelphia, PA, USA, 1985.

Liou, K.: Influence of cirrus clouds on weather and climate processes: a global perspective, Mon. Weather Rev., 114, 1167–1199, 1986.

Liu, X. and Penner, J. E.: Ice nucleation parameterization for global models, Meteorol. Z., 14, 499–514, 2005.

Marcolli, C., Gedamke, S., Peter, T., and Zobrist, B.: Efficiency of immersion mode ice nucleation on surrogates of mineral dust, Atmos. Chem. Phys., 7, 5081–5091, 2007, http://www.atmos-chem-phys.net/7/5081/2007/.

Meyers, M. P., DeMott, P. J., and Cotton, R.: New primary ice-nucleation parameterization in an explicit cloud model, J. Appl. Meteorol., 31, 708–721, 1992.

Minnis, P.: Contrails, cirrus trend, and climate, J. Climate, 17, 1671–1685, 2004.

Möhler, O., Büttner, S., Linke, C., Schnaiter, M., Saathoff, H., Stetzer, O., Wagner, R., Krämer, M., Mangold, A., Ebert, V., and Schurath, U.: Effect of sulfuric acid coating on heterogeneous ice nucleation by soot aerosol particles, J. Geophys. Res., 110, D11210, doi:11210.11029/12004JD005169, 2005.

Möhler, O., Field, P. R., Connolly, P., Benz, S., Saathoff, H., Schnaiter, M., Wagner, R., Cotton, R., Krämer, M., Mangold, A., and Heymsfield, A. J.: Efficiency of the deposition mode ice nucleation on mineral dust particles, Atmos. Chem. Phys., 6, 3007–3021, 2006, http://www.atmos-chem-phys.net/6/3007/2006/.

Monier, M., Wobrock, W., Gayet, J. F., and Flossman, A.: Development of a detailed microphysics cirrus model tracking aerosol particles histories for interpretation of the recent INCA campaign, J. Atmos. Sci., 63, 504–525, 2006.

Nenes, A. and Seinfeld, J. H.: Parameterization of cloud droplet formation in global climate models, J. Geophys. Res., 108, 4415, doi:4410.1029/2002JD002911, 2003.

Penner, J. E., Lister, D. H., Griggs, D. J., Dokken, D. J., and McFarland, M.: Aviation and the global atmosphere - A special report of IPCC working groups I and III. Intergovernmental Panel on Climate Change, Cambridge University Press, 365 pp., 1999.

Peter, T.: Microphysics and heterogeneous chemistry of polar stratospheric clouds Annu. Rev. Phys. Chem., 48, 785–822, 1997.

Phillips, V. T. J., Donner, L. J., and Garner, S. T.: Nucleation processes in deep convection simulated by a cloud-system-resolving model with double-moment bulk microphysics, J. Atmos. Sci., 64, 738–761, doi:710.1175/JAS3869.1171, 2007.

Phillips, V. T. J., DeMott, P. J., and Andronache, C.: An empirical parameterization of heterogeneous ice nucleation for multiple chemical species of aerosol, J. Atmos. Sci., 65, 2757–2783, doi:2710.1175/2007JAS2546.2751, 2008.

Prenni, A. J., DeMott, P. J., Twohy, C. H., Poellot, M. R., Kreidenweis, S. M., Rogers, D. C., Brooks, S. D., Richardson, M. S., and Heymsfield, A. J.: Examinations of ice formation processes in Florida cumuli using ice nuclei measurements of anvil ice crystal particle residues, J. Geophys. Res., 112, D10121, doi:10110.11029/12006JD007549, 2007.

Pruppacher, H. R. and Klett, J. D.: Microphysics of clouds and precipitation 2nd ed., Kluwer Academic Publishers, Boston, MA 1997.

Ren, C. and Mackenzie, A. R.: Cirrus parameterization and the role of ice nuclei, Q. J. Roy. Meteorol. Soc., 131, 1585–1605, doi:10.1256/qj.04.126, 2005.

Sassen, K., DeMott, P. J., Prospero, J. M., and Poellot, M. R.: Saharan dust storms and indirect aerosol effects on clouds: CRYSTAL-FACE results, Geophys. Res. Lett., 30, 1633, doi:1610.1029/2003GL017371, 2003.

Seinfeld, J. H.: Clouds, contrails and climate, Nature, 391, 837–838, 1998.

Spichtinger, P. and Gierens, K. M.: Modelling of cirrus clouds – Part 2: Competition of different nucleation mechanisms, Atmos.

Chem. Phys., 9, 2319–2334, 2009, http://www.atmos-chem-phys.net/9/2319/2009/.

Tabazadeh, A., Jensen, E. J., and Toon, O. B.: A model description for cirrus cloud nucleation from homogeneous freezing of sulfate aerosols, J. Geophys. Res., 102, 23485–23850, 1997a.

Tabazadeh, A., Toon, O. B., and Jensen, E. J.: Formation and implications of ice particle nucleation in the stratosphere, Geophys. Res. Lett., 24, 2007–2010, 1997b.

Vali, G.: Freezing rate due to heterogeneous nucleation, J. Atmos. Sci., 51, 1843–1856, 1994.

Vali, G.: Repeatability and randomness in heterogeneous freezing nucleation, Atmos. Chem. Phys., 8, 5017–5031, 2008, http://www.atmos-chem-phys.net/8/5017/2008/.

Waliser, D. E., Li, J. F., Woods, C. P., Austin, R. T., Bacmeister, J., Chern, J., Del Genio, A. D., Jiang, J. H., Kuang, Z., Meng, H., Minnis, P., Platnick, S., Rossow, W. B., Stephens, G. L., Sun-Mack, S., Tao, W., Tompkins, A. M., Vane, D. G., Walker, C., and Wu, D.: Cloud ice: A climate model challenge with signs and expectations of progress, J. Geophys. Res., 114, D00A21, doi:10.1029/2008JD10015, 2009.

Welti, A., Lüönd, F., Stetzer, O., and Lohmann, U.: Influence of particle size on the ice nucleating ability of mineral dusts, Atmos. Chem. Phys. Discuss., 9, 6929–6955, 2009, http://www.atmos-chem-phys-discuss.net/9/6929/2009/.

Zobrist, B., Koop, T., Luo, B., Marcolli, C., and Peter, T.: Heterogeneous ice nucleation rate coefficient of water droplets coated by a nonadecanol monolayer, J. Phys. Chem. C, 111, 2149–2155, 2007.

Zobrist, B., Marcolli, C., Peter, T., and Koop, T.: Heterogeneous ice nucleation in aqueous solutions: the role of water activity, J. Phys. Chem. A, 112, 3965–3975, 2008.

Zuberi, B., Bertram, A. K., Cassa, C. A., Molina, L. T., and Molina, M. J.: Heterogeneous nucleation of ice in $(NH_4)_2SO_4$-H_2O particles with mineral dust immersions, Geophys. Res. Lett., 29, 1504, doi:1510.1029/2001GL014289, 2002.